Title: Functionally graded materials with a soft surface for improved indentation resistance: Layout and corresponding design principles.

Authors:

- **Tobias Ziegler (Corresponding Author)**

  Fraunhofer Institute for Mechanics of Materials, Wöhlerstraße 11, D-79108 Freiburg, Germany; +49 761 5142 367; Tobias.Ziegler@iwm.fraunhofer .de

- **Torsten Kraft**

  Fraunhofer Institute for Mechanics of Materials, Wöhlerstraße 11, D-79108 Freiburg, Germany; Torsten.Kraft@iwm.fraunhofer .de

Abstract:

We report the finding of an optimal layout of functionally graded materials (FGM) towards indentation resistance. This optimum is characterized by a minimum in tensile surface stresses that can lead to a belated onset of cracking compared to homogeneous materials of uniform stiffness. The parameters influencing the tensile surface stresses in a FGM consisting of a soft surface layer, a stiff base material and a graded region between them have been investigated by finite element analysis and an optimum is reported for the first time. The results in general units can be used to design the gradient in any FGM from plastics to ceramics to result in low tensile surface stresses for a given load.

Keywords:

Smart materials; Mechanical properties; Finite element analysis (FEA); Functionally Graded Materials (FGM)

1. Introduction

Functionally graded materials (FGMs) have first been investigated in Japan in the 1980s during the Hope-X space plane research project and have since become a major area of research in materials science. Since the mid 90s the amount of papers published in this area has increased from around 100 papers to almost 1000 papers per year. Applications range from design to medical applications [1] to FGMs for improved tribological properties [2,3].

A wide variety of production techniques has been developed including rapid manufacturing machines [4]. This allows for easy production with a lot of freedom in the layout, which poses the question: "How should we design FGMs for a given function?"

A typical load situation is indentation into functionally graded half spaces. One of the first theoretical studies by Giannakopoulus and Suresh [5] studied the contact problem for FGMs with a graded exponential law. Ke and Wang [6] have developed a multi-layer model to numerically solve the contact problem for arbitrary variations in stiffness. This model These covers the direct area of contact. Experimental evidence for benefits of graded substrates towards indentation has been given by Jitcharoen et. al. [7], who showed that the creation of Hertzian cracks under indentation can be supressed in graded materials. This gives great opportunities to design FGMs for increased usability under indentation.

Similar load cases often occur in tribological applications where the indented half space is typically moved under the indenter. For example, shoe soles or tires could increase their durability on uneven terrain. As these examples show general design rules for FGMs with improved resistance towards indentation can be applied to a wide range of materials from plastics to ceramics.

While the possible benefits of well-designed FGMs have been proven experimentally and described theoretically by Jitcharoen et. al. [7], no thorough study of the parameters

involved on the resulting stresses has been given up to date. Therefore, we studied this phemomenon in detail and present a finite element (FE) study of the influence of gradients in material stiffness on the stresses developing during indentation with a rigid spherical indenter. The focus is set on tensile surface stresses, which are most likely to initiate damage and lead to failure. While the actual mode of damage will most certainly depend on the type of material, we try to give insight into general principles that can be applied to a wide range of different materials. The possible applications have shown that improved indentation resistance can be useful for virtually all materials available.

For most production methods a FGM will be made from two materials with differing stiffness layered on top of each other and a graded volume in between where the stiffness smoothly changes from one material's to the other's. This layout was chosen as being most useful for engineers designing FGMs. Depending on the production method of the FGM internal stresses are likely to be present. As these strongly depend on the material and the production method employed they are left out of the current analyses. Possible residual stresses can be superimposed if necessary due to the assumed linear elasticity.

2. Method

Analytical solutions would be rather complex if existing at all. Therefore, we have used finite elements for the analysis. They have the advantage of being easily customizable and all information of interest is easily accessible. This includes stresses at the surface as well as inside of the FGM. FEA is especially suited for parameter analysis like the ones presented here where many calculations have to be performed.

2.1. Our Setup

As we have pointed out the aim of this study is to give insights how to design a FGM for

improved resistance towards indentation. As the parameter space is very large for this type of problem we had to make a number of assumptions. The emphasis was set on giving general insight that does not depend on a certain type of material. The assumptions that have been made are:

- No residual stresses exist
- Linear elasticity is assumed together with isotropic material behaviour
- The spherical indenter is rigid
- Frictionless contact is assumed

The ABAQUS/Standard finite element program was used [8]. For the parameter study a mesh with 24524 eight-noded 2^{nd} order axisymmetric elements was used. The indenter was taken as a rigid body. Please note that the maximum contact pressure as well as the resulting force was sensitive to the domain size in depth direction, while the tensile surface stress and the contact radius were susceptible to the domain size in radial direction. The outer boundaries were taken to be at least 50 times the contact radius to account for these findings (**Figure 1**). Along KL symmetric boundary conditions have been applied. Along LM the movement was restricted along the z-axis. All other boundaries had no conditions applied to them.

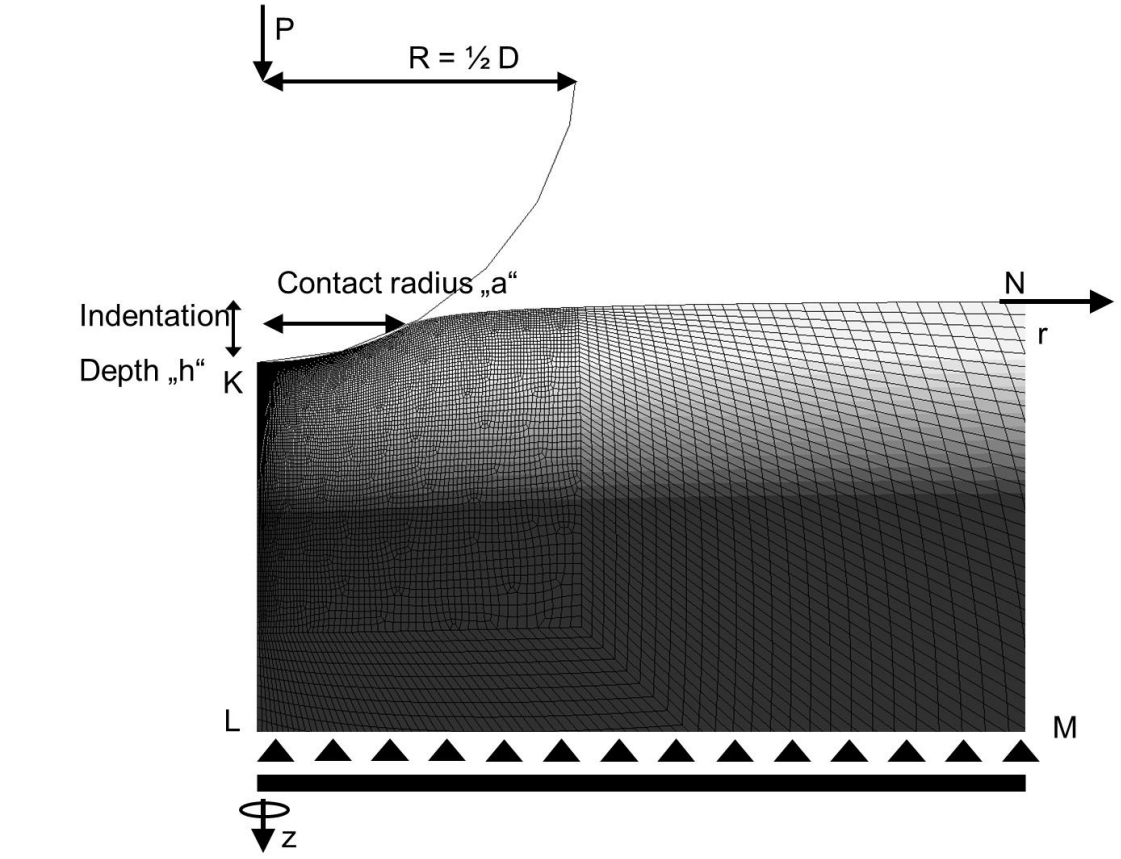

Figure 1: Setup of the FEA. The indenter is visible on the top left and pressed down the distance “h” with the Force “P” which results in a contact radius “a”. The four points K, L, M and N are used to define boundary conditions imposed on the setup.

Typically more than 100 elements were in contact during the analysis to give a sufficient resolution for the stresses inside and outside of the contact region.

The gradient depth β was defined as the depth at which the stiffness is the mean value of the two materials (see **Figure 2**). For linear gradients the gradient length Δ defines the distance over which the stiffness changes from the surface material to the base material.

As a convergence test the amount of elements was quadrupled and the influence on the results investigated. The resulting force was equal to the fourth digit; the contact pressure was within 1‰. The maximum principal tensile stress at the surface was along radial direction and its variation less than 1%.

To model gradients in material stiffness the stiffness was set at every integration point according to its depth z. Thus, the resolution was not limited to element size and artificial shear stresses between layers could be avoided.

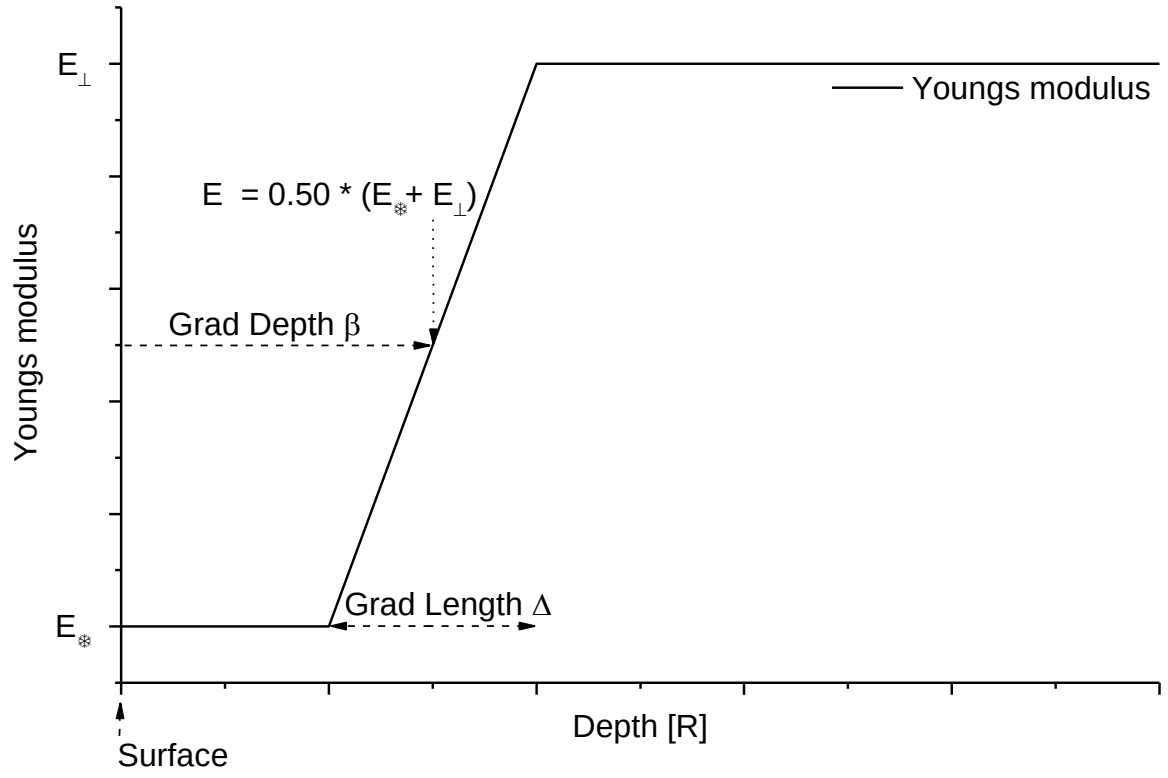

Figure 2: The Young's modulus of the FGM is here varying linearly from $E_{\top}$ at the surface to E⊥ at the bottom over a distance called Grad Length Δ. The change in stiffness takes place at Grad Depth β which is defined as the depth at which the stiffness is the average of $E_{\top}$ and E⊥.

2.2. Verification

For comparison the results from Suresh et al. [9] have been reproduced. For this the Young's modulus was varied as a function of the depth -z according to following equation: $E = E_0 e^{-\alpha z}$

where 1/α is a length parameter. Calculations were performed for α = -0.5; -0.25; 0; 0.25;

0.5 all given in units of R/2. The resulting P-h curves are shown in **Figure 3**. Our results for these special cases are close to the ones obtained by Suresh et al. However, for α below zero we had to apply additional boundary conditions which were not mentioned in [9] restricting movement along MN (**Figure 1**). If this condition was not applied the stiff surface layer would compress the compliant base layer without curvature at the contact region.

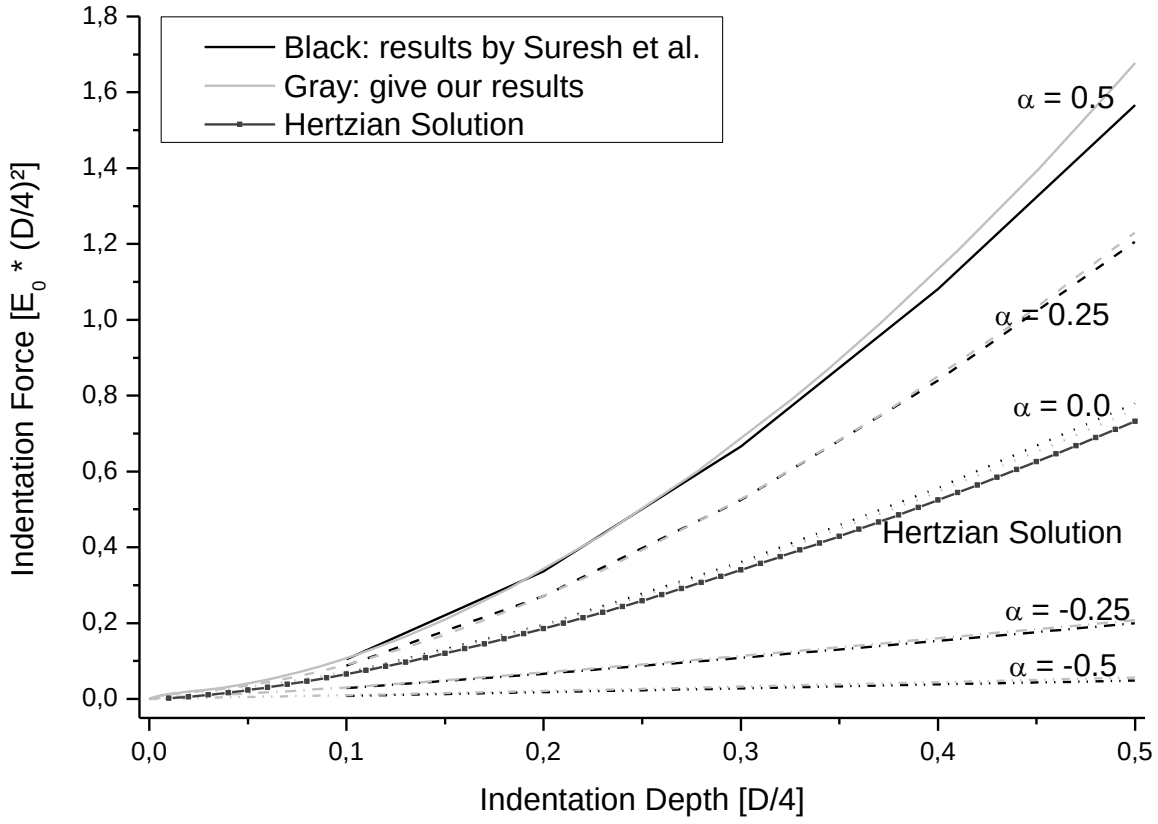

Figure 3: Reproduction of the results from Suresh et al. [9]. P-h curves for spherical indentation into functionally graded materials with an exponential stiffness-depth profile.

For the Hertzian case (α = 0.0) our result is closer to the analytical solution. More results are given in Table **1**. Most results compare well except the maximum tensile principal stress $(\sigma_1)_{max,}$ which is one order of magnitude higher. Although we have no proof we attribute this discrepancy to a wrong position of the decimal point.

Parameter α (D/4)	-0.5	-0.25	0	0.25	0.5

Contact Radius $a/(D/4)$	0.46 / 0.44	0.71 / 0.67	1.08 / 0.99	1.17 / 1.11	1.21 / 1.16
Applied Force $P/(E_0(D/4)^2)$	0.0486 / 0.0565	0.2 / 0.208	0.78 / 0.76	1.21 / 1.23	1.57 / 1.68
Maximum Contact Pressure p_{max}/ E_0	0.125 / 0.136	0.212 / 0.221	0.392 / 0.391	0.537 / 0.536	0.678 / 0.686
Maximum Mises Effective Stress $(\sigma_e)_{max}/ E_0$	0.0702 / 0.0782	0.119 / 0.131	0.267 / 0.246	0.424 / 0.352	0.579 / 0.463
Maximum Tensile Principal Stress $(\sigma_1)_{max}/ E_0$	0.00135 / 0.0137	0.0019 / 0.0281	0.00567 / 0.0598	0.00791 / 0.0736	0.00842 / 0.0841

Table 1: Comparison of our results (gray bottom right corner) with data by Suresh et. al. [9] (black top left corner).

3. Results:

Now we present our results which are aimed at giving the reader a set of rules at hand how to design a FGM for optimal resistance towards indentation. For all simulations performed the material with the higher Young's modulus was always the substrate at the bottom i.e. $E_{\top} < E_{\perp}$. This was chosen because of the results from Suresh et al. [9], who found a reduction in tensile surface stresses for this setup. All resulting stresses are given relative to the bottom materials Young's modulus $E_{\perp}$. A range of parameters were varied. These parameters include the gradient depth β, force of indentation, gradient length Δ, ratio of the materials Young's moduli and the Poisson ratio. For the reference setup the ratio between surface and base material stiffnesses was chosen to be two. Similarly the Poisson ratio μ is assumed to be 0.33.

As a first step, various gradient midpoints and forces of indentation were investigated. For these simulations $\Delta = 0$ was set. This is equivalent to a two layer material with no gradient at all. The results are shown in **Figure 4**. It can be seen that a certain gradient midpoint

exists which results in a minimum tensile stress. Shear stresses that might arise at the interface are ignored here and will be looked upon in later simulations with gradients.

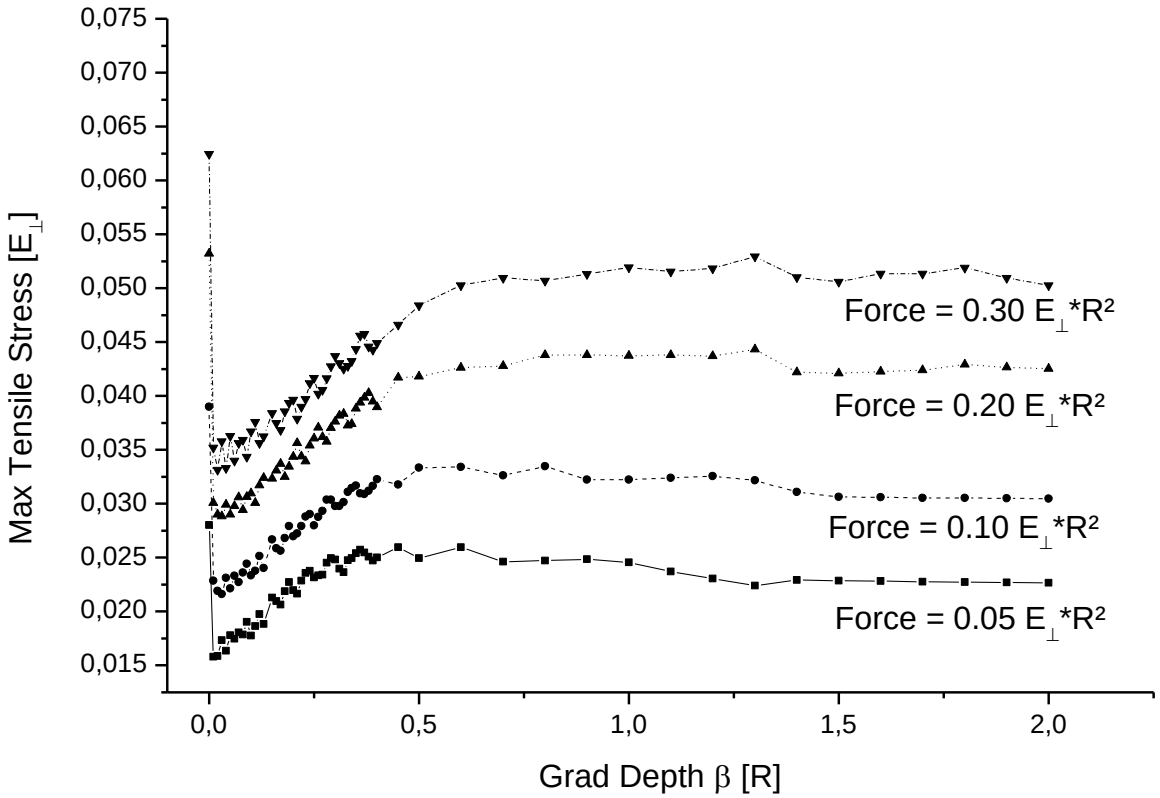

Figure 4: For a gradient length of zero the gradient midpoint was varied and the maximum tensile stresses were evaluated.

In a second simulation the force P was kept constant at 0.3 $E_\perp * R^2$ where again $E_\perp$ is the Young's modulus of the bottom material. Different Δ's were explored and their influence on the stress over β curves examined. The resulting graphs are shown in **Figure 5**.

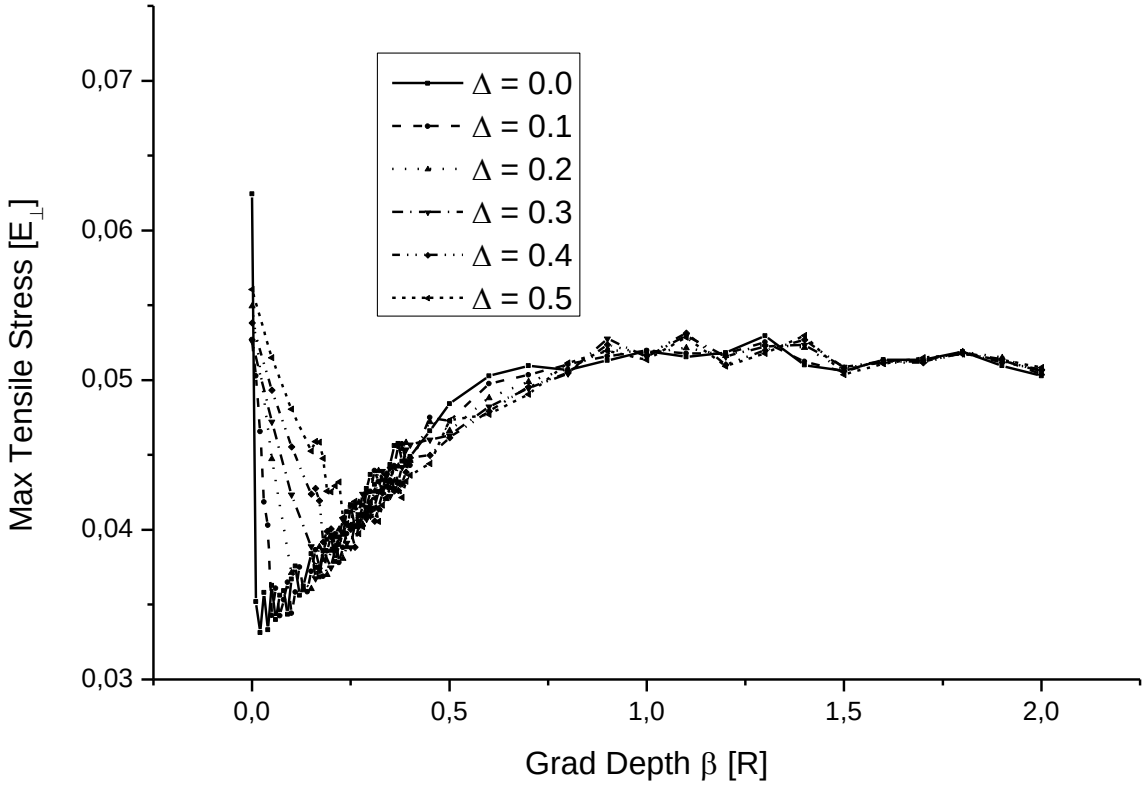

Figure 5: For a constant force P of 0.3 $E_{\perp}*R^2$ different gradient lengths Δ (all in units of R) were explored.

The next parameter to be varied was the ratio of the two material stiffnesses (Figure 6). Numerical stability limited the parameter space that could be explored here. The depth of the local minimum of the tensile stress increased dramatically with the spread in stiffness. The last variable to be analysed was the Poisson ratio. This was changed for both materials accordingly (Figure 7) and resulted in a constant absolute shift of the resulting graphs.

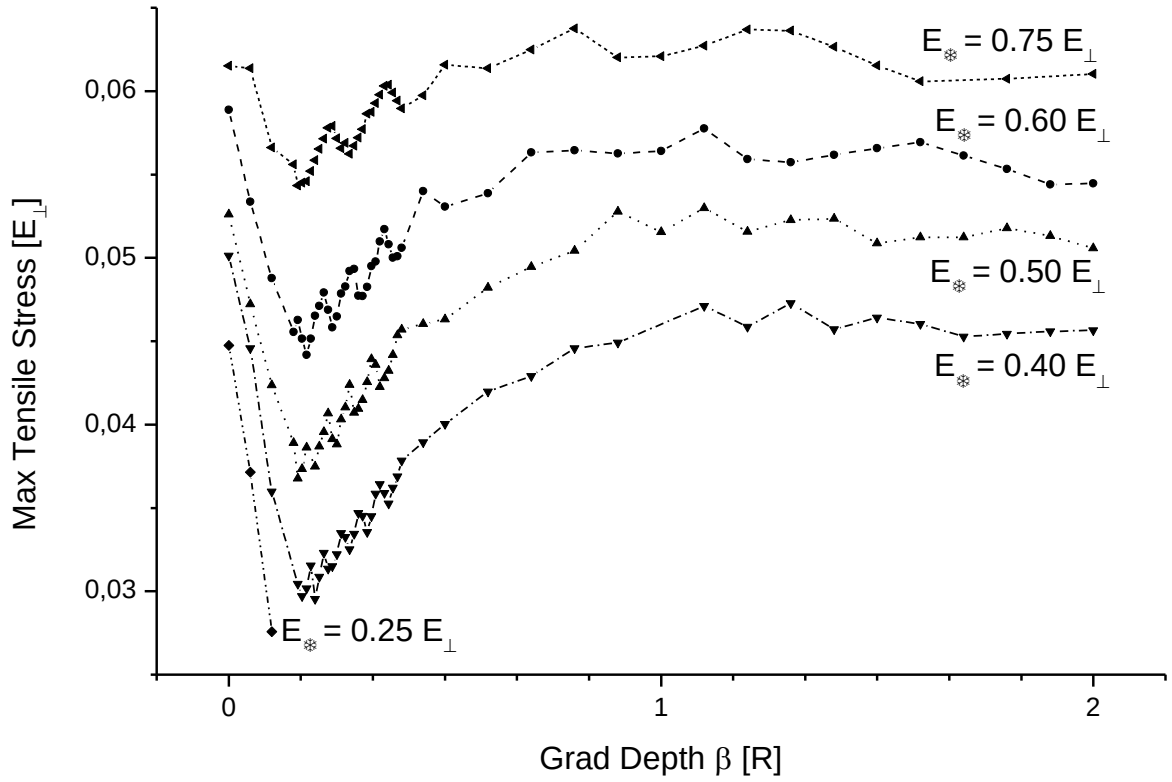

Figure 6: For a constant force of 0.3 $E_\perp * R^2$ and a constant gradient length of 0.3 R different ratios of the two material stiffnesses were investigated.

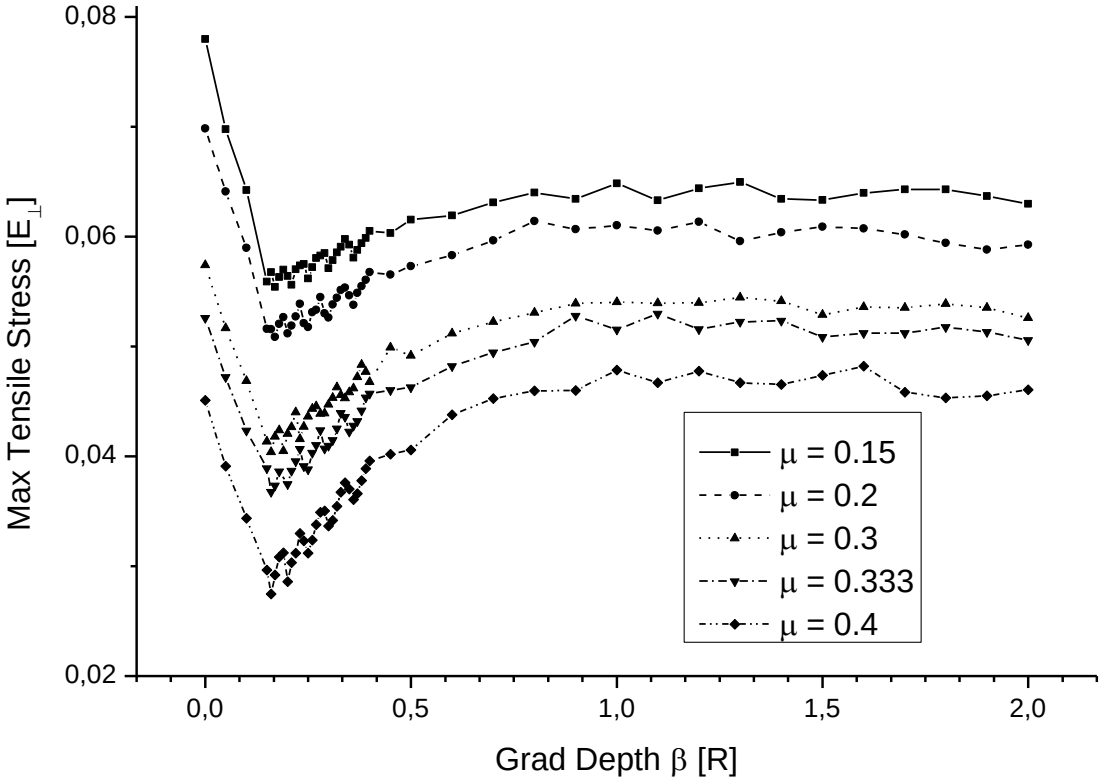

Figure 7: For a constant force of 0.3 $E_{\perp}*R^2$, a constant Δ of 0.3 R and a constant stiffness ratio of $E_{\top} = 0.5 * E_{\perp}$ the Poisson ratio of both materials was modified.

4. Discussion:

   The resulting tensile stresses at the surface exhibit a noticeable dependence on the gradient depth. While one might expect the stress to monotonously decrease from the higher value that might be expected for a solid material with constant higher stiffness (i.e. $\beta = 0$) to the lower value for a solid material with constant lower stiffness (i.e. $\beta = \infty$) this is not observed. Instead a local minimum is observed that is below the stress for a solid material with constant lower stiffness (i.e. $\beta = \infty$). This result, which has to our knowledge not been published before, sheds further light on the experimental findings of Jitcharoen et. al. [7]. If one assumes that crack initiation solely depends on the tensile surface stress then the observed reduction in said stress should make an adequately designed FGM much more fracture resistant to indentation. Many practical applications that might benefit

from this come easily to mind, eq. dental crowns. This is conceptually similar to shot peening, where compressive residual stresses are introduced at the surface [10] thus lowering the tensile surface stresses which prevents crack initiation. This works well and is applied for example in the aviation industry [11]. However this concept has its limitations, even if crack initiation at the surface can be prevented there are strength limits in the very high-cycle fatigue regime as shown by Shiozawa and Lu [12] who found that sub surface defects evolve into cracks which lead to failure.

As Δ is increased from zero upwards the ideal grad depth moves deeper inside the material (**Figure 5**). Within the parameter space tested ($E_{\top} = 0.5\ E_{\perp}$; $0 < \Delta/R < 0.5$; $\mu = 0.33$ and $P/(E_{\perp}*R^2) = 0.3$) the optimal Grad depth is approximately described by the linear relationship:

$$\beta_{opt} = 0.6 * \Delta$$

Equation 1: Optimal Grad Depth for varying Δ within the parameter space tested

The position of the optimal grad depth does not depend on the ratio of the two materials stiffnesses as well as the Poisson ratio (Figure 6 and Figure 7).

For a useful material the gradient length should be sufficiently large to prevent shear stresses inside the FGM from delaminating the two materials. To illustrate this, the in-plane shear stress distribution is shown in **Figure 8** for a homogeneous half space and a graded material with Δ=0.3 R, β = 0.18 R and a force of 0.3 $E_{\perp}*R^2$. The maximum values of the shear stresses are similar with 0.108 $E_{\perp}$ for the homogeneous material and 0.094 $E_{\perp}$ for the graded material. Within the graded material the maximum is placed further away from the surface and the area of highest stresses is smaller. We therefore suggest - within our reasoning that the tensile surface stresses are the cause of crack initiation and ultimately failure - that Δ does not have to be bigger than 0.3 R as the shear stresses within the material are comparable to a homogeneous material.

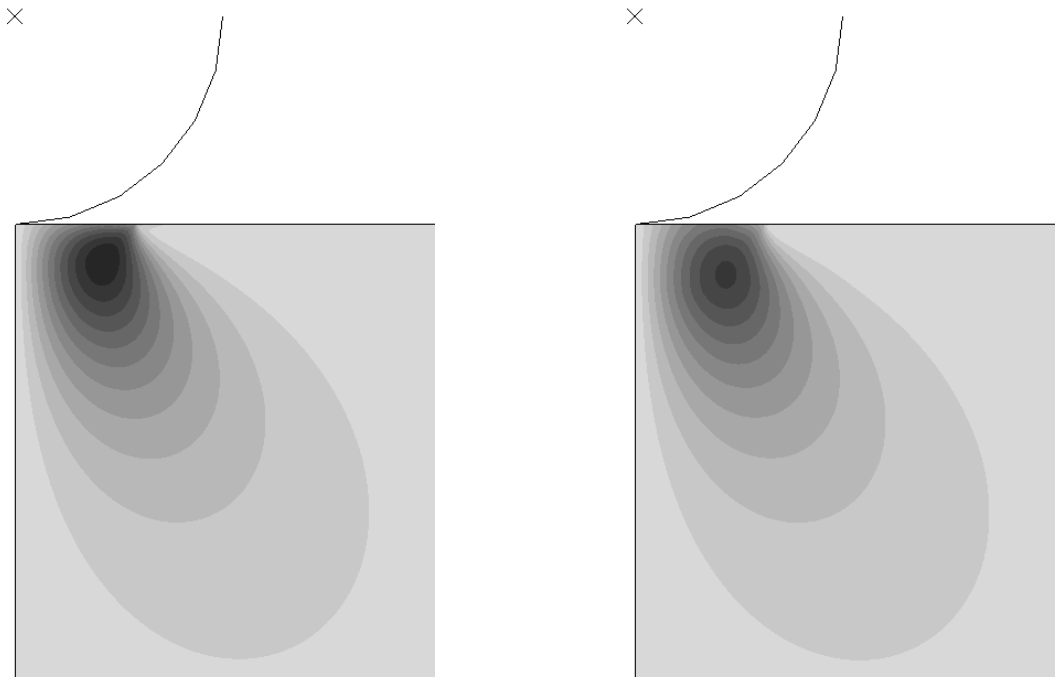

Figure 8 Left side: Distribution of the in-plane shear stress in a homogeneous half space. Right side: Distribution of the same shear stress in a graded half space with Δ=0.3 R and β = 0.18 R. The scale is the same on both sides.

The reduction in tensile surface stresses scales with the spread in the two materials stiffnesses. If possible the two materials should be chosen with as much of a disparity in their respective stiffnesses as possible. The Poisson ratio should be as large as possible. For most applications the choice of material will be very limited.

5. Summary

Materials with a graded stiffness can be designed to reduce the tensile stress at the surface during indentation. An FE study of the parameters involved was presented for a setup with a soft surface layer, a stiff base material and a graded region in between. The influence of parameters like gradient length, gradient depth, ratio of two materials stiffness and Poisson ratio on the resulting tensile surface stress was investigated. We have found that the tensile surface stress has a local minimum for a certain Gradient depth. All results are given in generalized numbers and can easily be scaled for any graded material from soft plastics to stiff ceramics. Within the parameter space tested we have presented a simple

formula (Equation) which yields the optimal position of the Gradient depth β as a function of the Gradient Length Δ. We further suggest that a Δ of more than 0.3 R is not necessary. The discrepancy in the two materials stiffnesses should be as large as possible while the Poisson Ratio should be as large as possible. With this information any engineer can design a FGM to optimally withstand spherical indentation of a specific.

[1] Oxman, N., 2011. Virtual and Physical Prototyping. Virtual Phys. Prototyp., **6**, 3–31

[2] Prchlik, L., Sampath, S., Gutleber, J., Bancke, G. and Ruff, A.W., 2001. Friction and wear properties of WC-Co and Mo-Mo2C based functionally graded materials. Wear, **249,** 1103–1115.

[3] Zhao, C., Vleugels, J., Vandeperre, L., Basu, B. and Van Der Biest, O., 1999. Graded Tribological Materials Formed by Electrophoresis. Mat. Sci. Forum, **308–311,** 95-100.

[4] Levy, G., Schindel, R. and Kruth, J.P., 2003. Rapid manufacturing and rapid tooling with layer manufacturing technologies: state of the art and future perspectives. CIRP Ann., **52,** 589–609.

[5] Giannakopoulos, A.E. and Suresh, S., 1997. Indentation of solids with gradients in elastic properties. Int. J. Solids Struct., **34,** 2357–2428

[6] Ke, L.L. and Wang, Y.S., 2006. Two-dimensional contact mechanics of functionally graded materials with arbitrary spatial variations of material properties. Int. J. Solids Struct., **43,** 5779–5798.

[7] Jitcharoen, J., Padture, N.P., Giannakopoulos, A.E. and Suresh, S., 1998, Hertzian Crack Suppression in ceramics with elastic modulus graded surfaces. J. Am. Ceram. Soc., **81,** 2301

[8] ABAQUS (2011) Finite Element Code, Version 6.10. SIMULIA Providence, RI.

[9] Suresh, S., Giannakopoulos, A.E. and Alcala, J., 1997. Spherical indentation of compositionally graded materials: theory and experiments. Acta. mater., **45,** 1307–1321

[10] Wang, S., Li, Y., Yao, M. and Wang, R., 1998. Compressive residual stress introduced by shot peening. J. Mater .Process. Technol., **73,** 64–73

[11] Friese, A., 2004. Worlds Largest Shot Peening Machine installed at Airbus Plant. Metal Finishing News, **5**

[12] Shiozawa, K. and Lu, L., 2002. Very high-cycle fatigue behaviour of shot-peened high-carbon-chromium bearing steel. Fatigue Fract. Engng. Mater. Struct., **25,** 813–822